Towards Material Modelling in Physical Models Using Digital Waveguides

Marc Aird*
Dept. Of Mathematical Sciences
University Of Bath

Joel Laird
Digital Music Research Group
University Of Bristol

Abstract

Digital Waveguides have been used extensively for musical instrument and room acoustics modelling. They can be used to form simplistic models for ideal wave propagation in one, two and three dimensions. Models in 1-d for string and wind instrument synthesis are now common and more recently a model for a drum, realised by creating an interface between 2-d and 3-d waveguide meshes, has been presented (Aird et al., 2000). A framework is thus in place for the virtual construction of any musical instrument, and indeed the design of new or abstract instruments. However straight-forward waveguides and waveguide meshes act in an extremely ideal nature, and phenomena such as stiffness and frequency dependent losses are often compromised or ignored altogether. In this paper we address these issues by considering extensions to the waveguide theory to incorporate material properties such as internal friction and elasticity. The models are introduced in the 1-d case for strings and bars, but could easily be extended to waveguide mesh models for stiff membranes and plates.

1 Introduction

This paper is divided in to five sections and introduces numerous areas of current research into physical modelling using digital waveguides. Firstly, in this introduction we quickly revise the definition of the digital waveguide and the lossless scattering junction. Following this we introduce the physical systems we wish to model. Sections three and four describe the models, and present simulation results and discussion, while the final section summarises the paper, and discusses the future directions that the authors wish to pursue.

A digital waveguide is simply a bi-directional delay line and is a discrete-time formulation of the travelling wave solution to the 1-d wave equation (Smith, 1992). For a junction of N waveguides, each with impedance R_i, where $i = 1, \ldots, N$ the junction velocity V_j may be written as,

$$V_j(n) = \frac{2\left(\sum_{i=1}^{N} R_i V_{j,i}^{+}(n)\right)}{\sum_{i=1}^{N} R_i}, \tag{1}$$

where $V_{j,i}^{+}$ is the incoming velocity from the i^{th} waveguide. Furthermore we write the outgoing velocity $V_{j,i}^{-}$ along the i^{th} waveguide as

$$V_{j,i}^{-}(n) = V_j(n) - V_{j,i}^{+}(n), \tag{2}$$

and observe that we may also calculate junction velocity from the outgoing velocities as

$$V_j(n) = \frac{2\left(\sum_{i=1}^{N} R_i V_{j,i}^{-}(n)\right)}{\sum_{i=1}^{N} R_i}.$$

2 Some Physical Properties of Strings and Bars

In this section we introduce some of the non-linearities inherent in the vibrations of real 1-d resonators and discuss elementary methods for including frequency dependent wave propagation speeds (dispersion) and losses.

2.1 Stiffness in Strings and Bars

The Digital Waveguide is derived by discretising the travelling wave solution to the 1-d wave equation

$$F\frac{\partial^2 y}{\partial x^2} = \rho\frac{\partial^2 y}{\partial t^2}, \tag{3}$$

where F is string tension and ρ is mass density per unit length. In this ideal formulation the only restoring force is due to tension and stiffness and internal friction are neglected. Furthermore all waves travel with the same speed $c = \sqrt{F/\rho}$. In an ideal beam there is no tension and the restoring force is due to stiffness. When the beam is struck, localised tension is introduced proportionally to the amount the beam is bent. The resultant partial differential equation (PDE) is

$$\frac{\partial^2 y}{\partial t^2} = -\frac{EI}{\rho A}\frac{\partial^4 y}{\partial x^4}, \tag{4}$$

where ρ, E is Young's modulus, A is the beam's cross-sectional area and I, the moment of inertia of the beam about it's perpendicular axis (Fletcher and Rossing, 1991)(Morse and Ingard, 1968). Note the 4^{th} order spatial derivative. This is the Euler-Bernoulli formulation for stiff bars which is considered a valid approximation in the low frequency range (Chaigne and Doutaut, 1997). By considering harmonic solution to (4) of the form $y = Ae^{j(kx-wt)}$

*mapma@maths.bath.ac.uk

we find that waves travel with a speed which varies with frequency according to $c(w) = \sqrt{w/a}$, where $a = \sqrt{\frac{\rho A}{EI}}$. Thus wave speed increases (from zero) with frequency. By adding a bar like term to (3) we may represent a stiff string as follows.

$$\frac{\partial^2 y}{\partial t^2} = \frac{F}{\rho}\frac{\partial^2 y}{\partial x^2} - \frac{EI}{\rho A}\frac{\partial^4 y}{\partial x^4}, \tag{5}$$

where now the restoring forces are due to tension and bending stiffness. Again by considering harmonic solutions to (5) we may derive a expression for the frequency dependent wave speed in a stiff string.

$$c(w)^2 = \frac{F}{2\rho} + \sqrt{\left(\frac{F}{2\rho}\right)^2 + \frac{\rho A}{EI}w^2}. \tag{6}$$

Note that when the stiffness is removed that (6) reduces to the case of the ideal string, and that when all tension is removed we reduce to the case of the ideal beam. We also note that for low frequencies the speed approximates that of the string, but that as frequency increases the speed of wave travel becomes more bar like. Finally, we observe that the introduction of a constant tension to a beam results in a non-zero wave speed at zero frequency.

2.2 A String on a Viscoelastic Foundation

In this short section we show how it is possible to add new terms to the PDE's described previously in order to introduce dispersion and frequency dependent loss. Firstly we consider placing a string on a purely elastic foundation, which may be thought of as laying the string on bed of springs (Graff, 1975). The governing equation is now

$$F\frac{\partial^2 y}{\partial x^2} - Gy = \rho\frac{\partial^2 y}{\partial t^2}, \tag{7}$$

where the new parameter is the foundation stiffness G. By again trying harmonic solutions we find the following relationship between frequency and wave number,

$$w^2 = c_0^2\left(k^2 + \frac{G}{F}\right), \tag{8}$$

where $c_0 = \sqrt{F/\rho}$ is the wave speed in the absence of foundation stiffness. By considering frequency against wave number we are able to predict both the fundamental frequency, and then the relative positions of each subsequent harmonic. A graph of this relationship is shown in Figure 1 and shows that the fundamental increases with frequency and that as the wavenumber increases, the resonant peaks will approach a harmonic series equivalent to the string in the absence of foundation stiffness.

We now propose a damped string obtained by including a resistive force to the motion resulting in the following governing equation,

$$F\frac{\partial^2 y}{\partial x^2} - g\frac{\partial y}{\partial t} = \rho\frac{\partial^2 y}{\partial t^2}, \tag{9}$$

where g is the resistive coefficient (Graff, 1975). This process can be thought of in the same terms as for the elastic

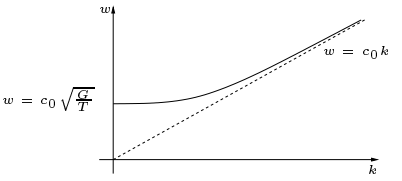

Figure 1: Frequency against wavenumber for a string on an elastic sub-base.

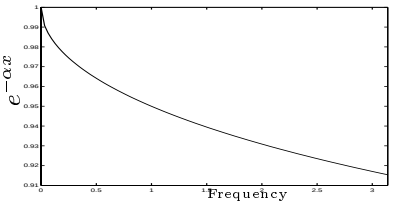

Figure 2: Freq-dependent Damping for String on Viscous Sub-Grade.

foundation, only with dash-pots replacing springs. This time however the damping prohibits the free propagation of harmonic waves, however we may consider solutions of the form $y = Ae^{-\alpha x}e^{j(kx-wt)} = Ae^{j[(k+j\alpha)x-wt]}$. Thus we have dispersive travelling waves which also include frequency dependent damping. Solving (9) for these solutions yields

$$k = M^{1/2}\cos(\phi/2),\ \alpha = M^{1/2}\sin(\phi/2), \tag{10}$$

for

$$M = \frac{w}{F}\left(g^2 + \rho^2 w^2\right)^{1/2},\ \phi = \tan^{-1}\left(\frac{g}{\rho w}\right).$$

We see that w will dominate for large values of the frequency, so that in any practical situation, the dispersion is minimal at low frequencies, and negligible elsewhere. We should also note that the damping term will cause damping of a lowpass nature. Shown in Figure 2 is the damping term for some typical simulation values.

3 Incorporating Bending Stiffness into Waveguide Models

In this chapter we investigate extensions to the Digital Waveguide in order to include the dispersion relationships found in stiff strings and vibrating beams. Stiffness in strings contributes to the 'twangy-ness', whilst for bars, an increase in the stiffness would result in more metallic tones. Previous work (Van Duyne and Smith, 1994a)(Van Duyne and Smith, 1994b) in this area has utilised Allpass filters (Laakso et al., 1996) placed at the waveguide terminations in order to introduce phase distortion, however these filters cannot be tuned precisely to match a true strings stiffness and cannot be used to model vibrating bars which exhibit zero wave speed at zero frequency. Thus we search for an all inclusive method which inherently models the so-called bending waves.

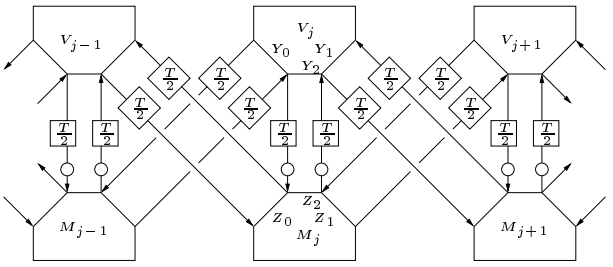

Figure 3: DWN for Euler-Bernoulli Bar.

3.1 Digital Waveguide Networks

A so-called Digital Waveguide Network (DWN) which models the Euler-Bernoulli bar was suggested in (Bilbao, 2001)(Bilbao, 2000). In this chapter we briefly describe the model and show it's equivalence to a stable finite difference scheme for the stiff wave equation introduced in Section 2. Consider decoupling equation (4) as follows

$$\frac{\partial v}{\partial t} = -\frac{1}{\rho A}\frac{\partial^2 m}{\partial x^2}, \tag{11}$$

$$\frac{\partial m}{\partial t} = EI\frac{\partial^2 v}{\partial x^2}. \tag{12}$$

In this equation v is the beam's transverse velocity, while m can be thought of as a bending moment. Using centred differences we arrive at the following difference scheme (FDS).

$$V_j(n+1) - V_j(n) =$$

$$-\frac{\mu}{\rho A}\left[M_{i+1}(n+\frac{1}{2}) - 2M_i(n+\frac{1}{2}) + M_{i-1}(n+\frac{1}{2})\right] \tag{13}$$

$$M_i(n+\frac{1}{2}) - M_i(n-\frac{1}{2}) =$$

$$\mu EI\left[V_{i+1}(n) - 2V_i(n) + V_{i-1}(n)\right], \tag{14}$$

where $\mu = \frac{T}{\Delta^2}$ for time step $T = \frac{1}{f_s}$ and spatial step Δ.

The proposed waveguide structure is shown in Figure 3. It is built from two coupled interleaved waveguides. To form an interleaved waveguide we split each unit of delay and place an extra junction in between the existing junctions in order to make available an alternative wave variable, in this case M. By using two interleaved waveguides placed one spatial step out of sync means we have have the two wave variables available at every spatial position. Intuitively this makes it possible to calculate the bending moment at each point, and we can see this happening through the coupling in Figure 3 where waves travelling to the moment junction from the velocity junction are multiplied by two, and halved travelling in the other direction.

Now, in order to derive an equivalence between the DWN structure of Figure 3 and the FDS of (13)(14) we require a little more information regarding the interleaved waveguides. In their original formulation, interleaved waveguides carried voltage and current waves (Bilbao, 2000) and in their use here V is assumed to be voltage-like, while M is the current like variable. If we denote a left-going wave by superscripting with a (+) and a right going wave with a (-) then

$$\begin{aligned} M^+ &= YV^+ \\ M^- &= -YV^-, \end{aligned}$$

where Y is the waveguide impedance, with admittance $Z = 1/Y$. Furthermore, in an interleaved delay line, the incoming waves to a scattering junction j can be expressed as the outgoing waves at neighbouring junctions in the following way for current-like waves,

$$\begin{aligned} M^+_{0,j}(n) &= -M^-_{1,j+1}(n-\frac{1}{2}), \\ M^-_{1,j}(n) &= -M^-_{0,j-1}(n-\frac{1}{2}), \end{aligned} \tag{15}$$

and for voltage-like waves,

$$\begin{aligned} V^+_{0,j}(n) &= V^-_{1,j+1}(n-\frac{1}{2}), \\ V^-_{1,j}(n) &= V^-_{0,j-1}(n-\frac{1}{2}). \end{aligned} \tag{16}$$

That is current-like waves travel with a sign inversion. Now beginning with a moment like junction we have

$$M_j(n+\frac{1}{2}) = \frac{2}{Z_j}\left(\tilde{V}^+_{,j}(n+\frac{1}{2}) + \tilde{V}^+_{1,j}(n+\frac{1}{2}) + \tilde{V}^+_{2,j}(n+\frac{1}{2})\right),$$

where $\tilde{V}^+_{l,j} = Z_l M^+_{l,j}$ represents incoming velocity to the moment junction, and is superscripted by a tilde so as to disassociate it with the incoming velocity to the velocity junction at the same time step. Note how the total junction velocity and total junction current can both be calculated using (1). Now using the relationships (2), (15) and (16) repeatedly, and noting that $\tilde{V}^-_{l,j} = -Z_l M^-_{l,j}$, we have,

$$\begin{aligned} M_j(n+\frac{1}{2}) &= \frac{2}{Z_j}\left[V^-_{1,j-1}(n) + V^-_{0,j+1}(n) - 2V^-_{2,j}(n)\right] \\ &= \frac{2}{Z_j}\left[V_{j-1}(n) + V_{j+1}(n) - 2V_j(n)\right] \\ &- \frac{2}{Z_j}\left[V^+_{1,j-1}(n) + V^+_{0,j+1}(n) - 2V^+_{2,j}(n)\right] \\ &= \frac{2}{Z_j}\left[V_{j-1}(n) + V_{j+1}(n) - 2V_j(n)\right] \\ &- \frac{2}{Z_j}\left[\tilde{V}^-_{0,j}(n-\frac{1}{2}) + \tilde{V}^-_{1,j}(n-\frac{1}{2}) + \tilde{V}^-_{2,j}(n-\frac{1}{2})\right] \\ &= \frac{2}{Z_j}\left[V_{j-1}(n) + V_{j+1}(n) - 2V_j(n)\right] \\ &+ M_j(n-\frac{1}{2}), \end{aligned}$$

which is identical to (14) if we set the total admittance at the moment junction to

$$Z_j = Z_0 + Z_1 + Z_2 = \frac{2}{EI\mu}.$$

We may similarly start from a velocity junction to arrive at a the following requirement for total velocity junction impedance

$$Y_j = Y_0 + Y_1 + Y_2 = \frac{2\rho A}{\mu}.$$

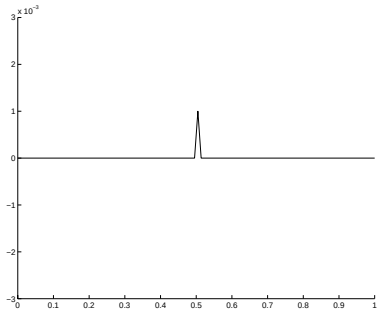

Figure 4: Evolution of transverse displacement waves along Euler-Bernoulli Bar, $t = 0$

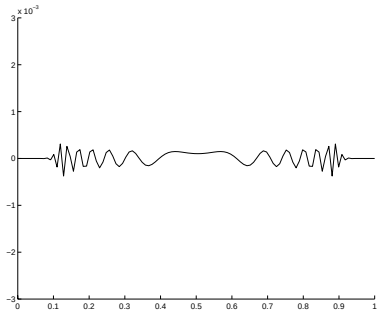

Figure 5: Evolution of transverse displacement waves along Euler-Bernoulli Bar, $t = 7.03 \times 10^{-4}$

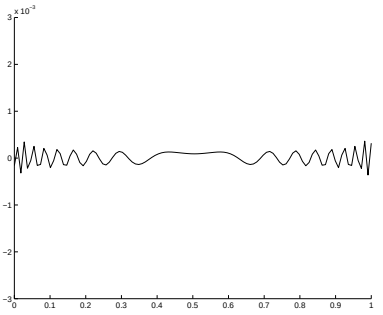

Figure 6: Evolution of transverse displacement waves along Euler-Bernoulli Bar, $t = 8.84 \times 10^{-4}$

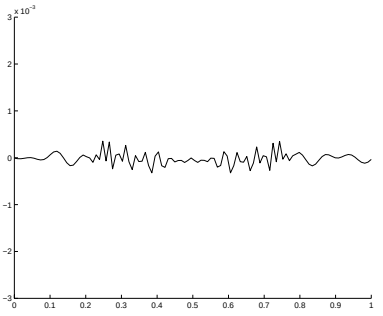

Figure 7: Evolution of transverse displacement waves along Euler-Bernoulli Bar, $t = 2.22 \times 10^{-3}$

Thus the DWN of Figure 3 is entirely equivalent to the FDS of (13)(14) and is hence a stable numerical scheme for the Euler-Bernoulli equation (4).

We carried out the following simulation to test the performance of the proposed model. We chose to model a steel bar with the following characteristics,

$$E = 1.4 \times 10^{12} N/m^2,$$
$$\rho = 5.38 \times 10^{4} kg/m^3,$$

with a square cross section of height $h = 0.005m$. This results in a step size of approximately $\Delta = 1/55m$ when the sample rate is set to $f_s = 44100Hz$, and we consider modelling a bar of length $1m$. Notice that we have chosen a bar with a very small cross-section. This has been done so as to keep the required sample rate down for the purposes of demonstration. Shown in Figures 4 to 7 is the time evolution of transverse displacements along the bar of our simulation which has fixed ends which are allowed to pivot and when the model is excited with an impulse. The model clearly exhibits a frequency dependent speed of wave propagation, with the higher frequencies reaching the boundary first. Also, the shape of the displacement is consistent with the expected displacements (Morse and Ingard, 1968). Finally we include a plot of frequency against harmonic index for our bar simulation in Figure 8. Notice how the shape of the curve is consistent with the expected curve which has k proportional to $\sqrt{w}$. Continued research by the authors on this model hopes to soon yield a simulation of a stiff string by treating the string as a thin stiff bar with circular cross section, held at a constant tension, however, this is out with the space constraints of this paper.

4 Material Modelling

It has been suggested that material modelling could be introduced into physical models by separately modelling shape and material (Djoharian, 1999)(Djoharian, 2000). Shape models could be attained using finite difference schemes, while the material could be implemented by *wearing the shape model with a viscoelastic dress.* Djoharian (Djoharian, 1999)(Djoharian, 2000) suggests that the material should be represented by using series-parallel combinations of springs and dashpots tuned to match a given materials viscoelastic response (Tschoegl, 1989)(Lakes, 1999). We have been investigating the use of digital waveguide as conservative models for the shape of a given resonator. For the material part, the simplest cases are when the resonator is placed on an elastic or viscous foundation, as described in Section 2.

4.1 Modelling the String on an Elastic Base

The string on an elastic base can be modelled by placing a self-loop of one unit of delay with a sign inversion at an extra port on each waveguide junction. We assume that the waveguide impedance is 1 while the self loop is

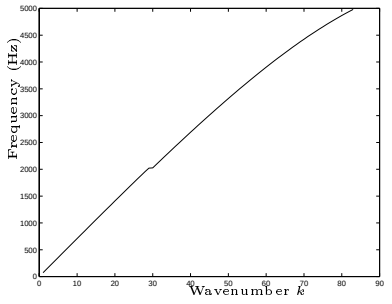

Figure 8: Frequency versus wavenumber for DWN bar model.

attached with impedance R_s. Beginning with the junction velocity equation for junction j, we have

$$\begin{aligned}
V_j(n) &= \frac{2}{R}\left[V^+_{j,1}(n) + V^+_{j,2}(n) + R_s V^+_{j,s}(n)\right] \\
&= \frac{2}{R}\left[V^-_{j-1,2}(n-1) + V^-_{j+1,1}(n-1) - R_s V^-_{j,s}(n-1)\right] \\
&= \frac{2}{R}\left[V_{j-1}(n-1) + V_{j+1}(n-1) - R_s V_j(n-1)\right] \\
&- \frac{2}{R}\left[V^+_{j-1,2}(n-1) + V^+_{j+1,1}(n-1) - R_s V^+_{j,s}(n-1)\right] \\
&= \frac{2}{R}\left[V_{j-1}(n-1) + V_{j+1}(n-1) - R_s V_j(n-1)\right] \\
&- \frac{2}{R}\left[V^-_{j,1}(n-2) + V^-_{j,2}(n-2) + R_s V^-_{j,s}(n-2)\right] \\
&= \frac{2}{R}\left[V_{j-1}(n-1) + V_{j+1}(n-1) - R_s V_j(n-1)\right] \\
&- V_j(n-2),
\end{aligned}$$

which is equivalent to

$$V_j(n+1) - 2V_j(n) + V_j(n-1) = \frac{2}{R}\left[V_{j-1}(n) - 2V_j(n) + V_{j+1}(n)\right] - 4\frac{R_s}{R}V_j(n),$$

where $R = 2 + R_s$ is the total junction impedance. Now, recalling equation (7) we may write a FDS for the system as

$$V_j(n+1) - 2V_j(n) + V_j(n-1) = \mu\frac{F}{\rho}\left[V_{j-1}(n) - 2V_j(n) + V_{j+1}(n)\right] - T^2\frac{G}{\rho}V_j(n),$$

where T is the time step, Δ is the spatial step, with $\mu = \frac{T^2}{\Delta^2}$. Thus we must fix

$$\begin{aligned}
\frac{2}{R} &= \frac{\mu F}{\rho}, \\
\frac{4R_s}{R} &= \frac{GT^2}{\rho}.
\end{aligned} \tag{17}$$

By fixing the time step T, then solving (17) gives

$$R_s = \frac{2GT^2}{4\rho - GT^2},$$

with spatial step

$$\Delta = \sqrt{T^2 F\left(\frac{4}{4\rho - GT^2}\right)}.$$

Stiffness G	Model Frequency	Real Frequency
0	96	96.1769
1	96	96.1776
10	96	96.1835
10^2	96	96.2427
10^3	97	96.8331
10^4	103	102.5501
10^5	148	148.0377
10^6	369	368.6482

Table 1: Comparing measured and real fundamental frequencies

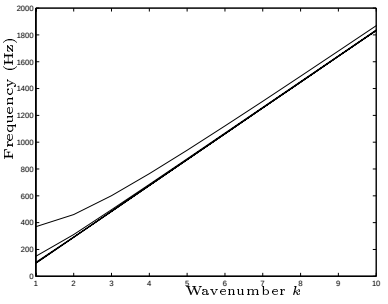

Figure 9: Frequency versus wavenumber for waveguide on a bed of springs.

We carried out an experiment for a string of length $L = 0.5m$ with density $0.2kg/m^2$ held at tension F N/m. The fundamental frequency (in Hz) of vibration may be calculated from

$$f_1 = \frac{c}{2\pi}\left[\left(\frac{\pi}{L}\right)^2 + \frac{G}{F}\right]^{\frac{1}{2}}.$$

Shown in Table 1 are the measured and expected fundamental frequencies for various values of the stiffness parameter G. All frequencies are measure in Hz and a high level of accuracy is attained. Furthermore we may also examine the dispersion properties by considering the positions of the resonant modes. Shown in Figure 9 shows plot of frequency against wavenumber for various values of G in our model. The fundamental frequency is that where the wave number is one and it clearly increases with increasing stiffness. We compare this graph to that of Figure 1 which shows the expected behaviour. At first each curve has zero gradient, but as the wave number k increases each curve approaches the straight line which represents the string in the absence of an elastic foundation.

4.2 Modelling the String on an Viscous Subgrade

We take a similar approach to that of the elastic foundation when modelling the string an a viscous subgrade given by (9). Again, we extend each waveguide junction to a 3-port, but this time the third junction receives a zero input signal. Thus the third port acts as a hole, out of which energy may seep. Now, again setting the waveguide impedance to

1 and this time setting the third impedance to R_d we may follow a similar formulation as before. This time we find that

$$V_j(n+1) - 2V_j(n) + V_j(n-1) = \frac{2}{R}\left[V_{j+1}(n) - 2V_j(n) + V_{j-1}(n)\right] - \frac{2R_d}{R}\left[V_j(n) - V_j(n-1)\right], \quad (18)$$

where this time $R = 2 + R_d$. Now clearly (18) is equivalent to a FDS for (9) if we set

$$\begin{aligned} \frac{2}{R} &= \frac{\mu F}{\rho}, \\ \frac{4R_s}{R} &= \frac{gT}{\rho}. \end{aligned} \quad (19)$$

Hence it is possible to introduce a physically reasonable loss to a digital waveguide. Traditionally losses have been added to digital waveguides by placing lowpass filters at the reflective terminations where the filters are designed to match measured losses. It is the authors' view that the method presented here could be extended to produce more physically relevant and controllable losses.

5 Conclusions and Future Research

In this paper we set out the requirements for the extension of the digital waveguide technique for the physical modelling of more realistic systems. We implemented a model of a waveguide bar, presenting encouraging results consistent with the literature, and indicated how it could be used for stiff strings. We then discussed how we could model more complicated material parameters and derived two models which introduced elementary phase distortion and frequency dependent losses in string models.

The models presented in this paper can be thought of as building blocks for complete instrument models. Once extended to include stiff strings, stiff membranes and plates, the interfacing procedure described in (Aird et al., 2000) would allow us to build complete instrument models. In the case of a drum for example, we may now create a realistic model for a membrane, which includes bending stiffness and material parameters for it's visco-elastic response. We can separately build a model for the drum shell made of wood or metal, say. The shell and membrane models are 2-d models, which can both be interfaced to the air column within the drum. Furthermore we would now be able to produce instruments made with materials not usually associated to them. For example, a drum shell could be made from ice or a xylophone with glass bars, which would not necessarily be possible in reality.

References

M. Aird, J. Laird, and J. Fitch. Modelling a drum by interfacing 2-d and 3-d waveguide meshes. In *Proceedings*. International Computer Music Conference, 2000.

Stefan Bilbao. Digital waveguide networks for inhomogeneous materials. In *Proc. of the 2nd COST G-6 Workshop on Digital Audio Effects DAFx99*, December 2000.

Stefan Bilbao. *Wave and Scattering Methods for the Numerical Integration of Partial Differential Equations*. PhD thesis, Stanford University, March 2001.

Antoine Chaigne and Vincent Doutaut. Numerical simulations of xylophones. i. time-domain modeling of the vibrating bars. *J. Acoust. Soc. Am.*, 101(1):539–557, 1997.

Pirouz Djoharian. Material design in physical modeling sound synthesis. In *Proc. of the 2nd COST G-6 Workshop on Digital Audio Effects DAFx99*, 1999.

Pirouz Djoharian. Shape and material design in physical modeling sound synthesis. In *Proceedings*. International Computer Music Conference, 2000.

N. H. Fletcher and T. D. Rossing. *The Physics Of Musical Instruments*. Springer-Verlag, New York, 1991.

Karl F. Graff. *Wave Motion in Elastic Solids*. Clarendon Press, Oxford, 1975.

T.I. Laakso, V. Valamaki, M. Karjalainen, and U.K. Laine. Splitting the unit delay - tools for fractional delay filter design. *IEEE Signal Processing Magazine*, 1996.

R.S. Lakes. *Viscoelastic Solids*. CRC Press, 1999.

P.M. Morse and K.I. Ingard. *Theoretical Acoustics*. McGraw-Hill, 1968.

J. O. Smith. Physical modelling using digital waveguides. *Computer Music Journal*, 16(4), 1992.

Nicholas W. Tschoegl. *The Phenomenological Theory of Linear Viscoelastic Behaviour*. Springer-Verlag, 1989.

S. A. Van Duyne and J. O. Smith. A simplified approach to modeling dispersion caused by stiffness in strings and plates. In *Proceedings*. International Computer Music Conference, 1994a.

S. A. Van Duyne and J. O. Smith. Travelling wave implementation of a lossless mode-coupling filter and the wave digital hammer. In *Proceedings*. International Computer Music Conference, 1994b.